View Article Online / Journal Homepage / Table of Contents for this issue
Dynamic Article Links

Journal of Materials Chemistry

Cite this: *J. Mater. Chem.*, 2012, **22**, 16698

www.rsc.org/materials

APPLICATION

Methane storage in metal organic frameworks

Kristina Konstas,*[a] Theresa Osl,[a] Yunxia Yang,[b] Michael Batten,[b] Nick Burke,[b] Anita J. Hill*[ac] and Matthew R. Hill[a]

Received 30th April 2012, Accepted 8th June 2012
DOI: 10.1039/c2jm32719h

In this applications article (116 references), the use and viability of metal organic frameworks (MOFs) for natural gas storage is critically examined through an overview of the current state of the field. These smart materials can be tuned to deliver best performance according to demand, as a function of temperature, desired storage pressure and mandated fill/release rates. Whilst the chemistry behind optimising natural gas storage performance in MOFs is highlighted, it is contextualised to the specific application in vehicular transport, and the best means of testing performance parameters are canvassed. Future applications of MOFs with natural gas are also discussed.

Published on 09 July 2012. Downloaded by CSIRO Library Services on 23/11/2015 04:48:30.

1. Introduction

Natural gas, which is predominantly methane, is set to be a key transitional fuel in the move from existing hydrocarbon-based fuels such as oil and coal, to renewable sources. It has a heat of combustion (methane $\Delta H^{298}_{comb} = -890$ kJ mol^{-1}),[1] and a higher hydrogen content than any other hydrocarbon fuel, meaning its carbon dioxide emissions relative to the energy generated from its combustion are also favourable. These factors, along with abundant worldwide reserves (see Fig. 1, bottom), mean there are inherent benefits for increased usage, and the development of new applications that utilise natural gas. Natural gas is predicted to undergo a drastic increase in demand over coming decades for energy production, due to factors that include its lower cost, local availability, cleaner combustion and greater competition for oil reserves (Fig. 1, top).[2] While natural gas may be converted to liquid transport fuels *via* Gas To Liquid (GTL) processes, natural gas in its neat form is an excellent substitute for diesel fuel[3,4] and the distribution network for natural gas is often well established through domestic pipeline networks. One of the present limitations to increased usage of natural gas is its low energy density and the consequent requirement to store the fuel either at very high pressures or as a liquid for such applications as natural gas powered vehicles. Liquefied Natural Gas (LNG) is a major breakthrough in storage, but is limited to systems where the implementation of large scale cryogenic storage vessels is

[a]*CSIRO Materials Science and Engineering, Private Bag 33, Clayton South MDCVIC, Australia, 3169. E-mail: Kristina.konstas@csiro.au; Fax: +61 3 9545 2837; Tel: +61 9545 7894*
[b]*CSIRO Earth Science and Resource Engineering, Private Bag 10, Clayton South MDCVIC, Australia, 3169*
[c]*CSIRO Process Science and Engineering, Box 312, Clayton SouthVIC, Australia, 3169*

Kristina Konstas

Dr Kristina Konstas completed her PhD in Organometallic Chemistry from Monash University (Australia) in 2007. Her studies focused on the synthesis of lanthanide and alkaline earth formamindate complexes. She joined the functional materials group at CSIRO in 2010 as a postdoctoral fellow. With a background in organometallic chemistry, her main research interests concerns the synthesis and functionalisation of porous (metal and covalent) frameworks for gas storage applications.

Theresa Osl

Ms Theresa Osl completed her Bachelor of Science in 2010 and is currently pursuing a MSc degree in the area of Organic and Biological Chemistry at the Technische Universität München, Germany. Her studies have taken her abroad to CSIRO where she has engaged in the synthesis of metal and covalent frameworks for gas storage applications.

This journal is © The Royal Society of Chemistry 2012

View Article Online

Published on 09 July 2012. Downloaded by CSIRO Library Services on 23/11/2015 04:48:30.

economically feasible.[4] Compressed Natural Gas (CNG) is a simpler storage method and indeed is in widespread application for vehicles in some Asian nations. Tank fill pressures of up to 300 bar are employed in these cases, requiring heavy storage vessels, and energy intensive compression of natural gas. Furthermore, the driving range of CNG vehicles is limited when compared to liquid fuels.[5] Nevertheless, the low cost, ready and often local availability of natural gas, along with its clean combustion makes it an attractive vehicle fuel. The ability to 'fill at home' would ameliorate to some extent the limitation of range of natural gas vehicles, particularly given that the majority of private vehicle trips are less than 50 km.[3,4] However, to encourage broader use of natural gas as a transport fuel, technologies that allow the lowering of pressures or the increase of quantities stored per volume are particularly attractive in the quest for increased usage of natural gas in vehicles.

Use of adsorbents within a storage tank offers the potential to drastically increase storage capacity, or lower the pressure for which a particular amount of natural gas can be stored. Physisorbents rely on adsorption to internal surfaces of a porous material, the strength of such an interaction being primarily governed by attraction between methane and the adsorbent surface. Of all the potential physisorbent materials, metal organic frameworks, MOFs, are the most promising. Consisting of metal atoms or clusters linked periodically by organic

Yunxia Yang

Dr Yunxia Yang completed her Bachelor degree at Sichuan University and Master degree at the Tsinghua University in China. After obtaining her PhD in the Department of Chemical Engineering at Monash University (Australia) in 2007, she joined CSIRO as a Research Scientist to work in the area of natural gas processing including gas storage and separation, conversion, adsorbent and catalyst development.

Michael Batten

Dr Michael Batten studied chemistry at Monash University (Australia) and at the University of Tasmania. In 2008 he completed his PhD studies in catalysts for the production of polyethylene plastics and synthetic oils. He has worked in the protective coatings and polymer industries, and as a chemical commodities market analyst (Reuters Data). Michael joined Johnson Matthey plc at their Royston Technology Centre in 2005. In 2008, he took a position with CSIRO where he works to develop gas processing and conversion technologies.

Nick Burke

Dr Nick Burke has a PhD in Chemical Engineering from the University of New South Wales (2001) and a Bachelors degree in Industrial Chemistry from the same institution. He joined CSIRO in 2001 as a post-doctoral fellow. Nick's main research interests are in the areas of natural gas processing and conversion with an emphasis on heterogeneous catalytic processes and gas storage and separation from the perspectives of chemistry and engineering.

Anita J. Hill

Dr Anita Hill obtained her PhD in Mechanical Engineering and Materials Science from Duke University. She is a Fellow of the Australian Academy of Technological Sciences and Engineering and an Office of the Chief Executive Science Leader at CSIRO Material Science and Engineering in active and adaptive materials. She is Chief of CSIRO Process Science and Engineering where she provides strategic leadership and implements policy to enable successful delivery of large scale multidisciplinary mission directed research programs addressing national challenges.

Matthew R. Hill

Dr Matthew Hill obtained his PhD in 2006 in inorganic materials chemistry from the University of New South Wales. Matthew joined CSIRO in 2006 to work in the area of porous materials. He leads a research team in energy and gas storage and also has interests in separations, with a particular focus on metal organic frameworks.

View Article Online

Published on 09 July 2012. Downloaded by CSIRO Library Services on 23/11/2015 04:48:30.

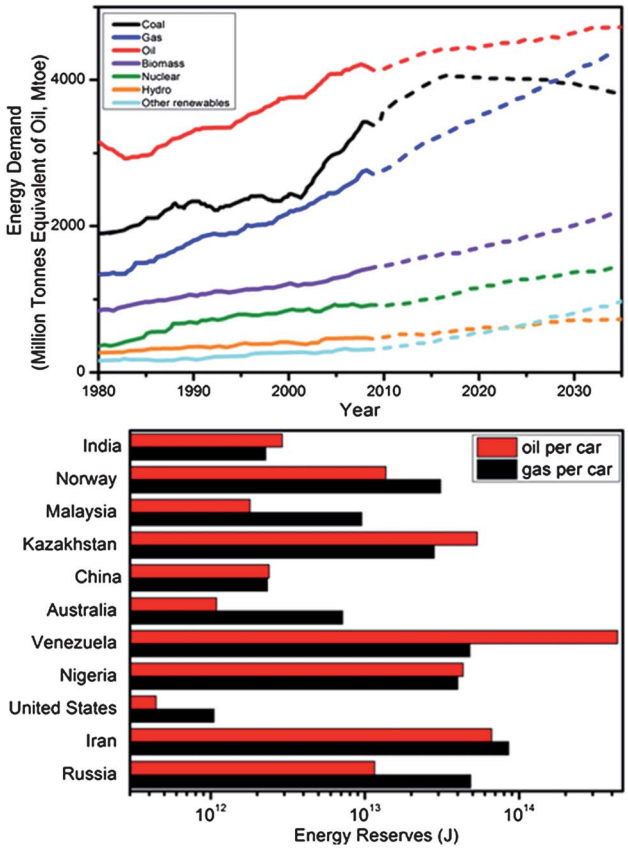

Fig. 1 There are nations worldwide that have significant natural gas reserves per vehicle, yet by and large only oil is used as a fuel (bottom).[2] Nevertheless, it is predicted that natural gas will overtake oil in energy demand in coming decades (top).[2]

molecules to establish an array where each atom forms part of an internal surface, MOFs have delivered the highest surface areas and methane storage capacities for any physisorbent. MOFs can act as smart materials for the storage of natural gas, with their surface chemistry and structure able to be tuned for a specific application, where performance criteria such as adsorption/desorption rate, capacity as a function of pressure, and operating temperature may be of particular importance. Exposed metal sites,[6] will increase storage capacities at low pressures, whereas increased pore sizes will improve uptake at high pressures.[7] Both of these parameters affect the enthalpy of adsorption within MOFs. Tuning the enthalpy of adsorption is one of the key methods of controlling performance parameters and is closely linked to the overall storage capacity. The 3-D interconnected pore architecture of many MOFs helps to maximise the adsorption and desorption rates by avoiding pore blockage.

The US Department of Energy (DOE) stipulates methane adsorption of 180 v/v at 298 K and 35 bar as the benchmark for adsorbed natural gas (ANG) technology,[8] and the optimum adsorption heat has been calculated at 18.8 kJ mol^{-1}.[9] Most of the recent research effort in methane storage materials has focussed on the development of porous carbons.[8] However, even the most sophisticated carbon structures struggle to significantly surpass the 180 v/v target,[8,10,11] largely because of the inherently low adsorption heat for methane within carbons, typically around 3–5 kJ mol^{-1}.[12] However, primarily due to the higher adsorption heats inherent to them, MOFs exhibit superior performance. Their periodic porosity allows for undiminished capacity upon cycling,[7,13] and they exceed the DOE target with the highest reported value currently being 230 v/v STP.[14]

Whilst MOFs offer great potential, more work is required to optimise their fast, low cost and large scale synthesis. Early progress using methods such as seeding,[15] microwave synthesis,[16] and autoclave preparations[17] are particularly encouraging and warrant further research on large scale production and application of MOFs.

This review describes the context for usage of MOFs for natural gas storage applications with a particular focus on use in vehicles, methods for measuring key performance parameters, and the effects of structure and surface chemistry on methane storage parameters. Future potential uses will also be discussed.

2. Strategies for enhanced methane storage in MOFs

As previously mentioned, the DOE has set the storage target by 2015 for CH_4 to be 180 v/v STP at 298 K and 35 bar.[8] Prior to MOF's, the benchmark material for methane sorption was activated carbon, with an uptake of about 200 v/v STP.[18]

First reports of methane uptake by a MOF were published by Kitagawa and co-workers in 1997 for the compound $[Co_2(4,4'\text{-}2,2'\text{-bipyridine})_3(NO_3)_4 \cdot 4H_2O]_n$ with an uptake of 77 v/v STP at 30 bar.[19] Studies have flourished since which have led to frameworks being designed with this specific purpose of methane uptake.[20] The current highest methane uptake MOF known is that reported by Zhou and co-workers for Cu_2(adip), adip = 5,5′-(9,10-anthracenediyl)di-isophthalate, known as PCN-14.[14] This MOF has a methane uptake of 230 v/v STP at 290 K and 35 bar, which is 28% higher than the DOE target. It is essential to exceed the DOE target in order to compensate for the MOF's low packing density which may greatly reduce their effective volumetric storage capacity when utilised in a tank.

Material chemistry as well as performance screening methods are both critical to the development of successful methane storage materials. Material properties of importance include capacity, enthalpy of adsorption, surface area, and porosity. This section of the review article presents strategies for designing the ideal methane sorbent material to meet or exceed DOE targets and covers both experimental and simulated MOF materials (Table 1).

2.1 Pore topology, pore size and surface area

Pore topology plays an important role in methane-accessible framework porosity. The metal coordination number and the functionality of di-, tri-, or multi-topic organic linker molecules combine to construct a framework with a predictable modular network.[21–23] The metal cluster vertices and the organic linkers self assemble during synthesis to form secondary building units (SBUs). To appreciate the influence of SBUs on pore size and porosity, the organic linker can be considered. The use of long linkers can increase the space between vertices, providing expanded structures with large pores. These MOFs commonly possess interpenetrated structures with a high surface area but as a consequence of interpenetration they have low porosity. In

 This journal is © The Royal Society of Chemistry 2012

View Article Online

Published on 09 July 2012. Downloaded by CSIRO Library Services on 23/11/2015 04:48:30.

Table 1 Summary of methane storage capacities in MOFs[a]

MOF		Surface area/m^2 g^{-1}		Methane storage				
		BET	Langmuir	Capacity v/v (STP) cm^3/cm^3	Q_{st} kJ mol^{-1}	*P* Bar	*T K*	Ref.
Mg–C_{60}@MOF	Mg–C_{60}@IRMOF-8			265[b]	13	35	298	28
Cu_2(adip)	PCN-14	1753	2176	230	30	35	290	32
Cu(OOC–Ph–CH=CH–COO)TED		3129		225			298	105
Cu(4,4′–OOC–Ph–Ph–COO)TED		3265		225	16.7		298	105
	NOTT-107	1770		196		35	298	27
Ni_2(DHTP)	Ni-MOF-74	1240		190	20.2	35	298	36
C_{60}@MOF	C_{60}@IRMOF-8			190[b]	11	35	298	28
Co_2(DHTP)	Co-MOF-74	1056		174	19.6	35	289	36
Cu_2(sbtc)	PCN-11	1931	2442	171	14.6	35	298	34
Zn_2(DHTP)	Zn-MOF-74	885		171	18.3	35	289	36
Zn_4O(1,2-DHCB-3,6-DC)	IRMOF-6	2804	3305	170		36	289	30
Zn_2(DOBDC)	Zn-MOF-74			170		35	298	6
CrOH(BDC)	MIL-53	1144		165		35	289	106
Cu_4(TDCPTM)	NOTT-140	2620		162	16.6	20	293	107
$Cu_3(BTC)_2$	HKUST-1	1502	2216	160	18.2	35	298	30
$CuSiF_6$(4,4′-BPY)			1337	159		36	289	108
Mn_2(DHTP)	Mn-MOF-74	1102		158	19.1	35	289	36
$Zn_4O(R_6BDC)_3$	IRMOF-6		2630	155		35	289	7
AlOH(BDC)	MIL-53-Al		1500	155		35	289	30
Cu_2(BDC)(DABCO)			1819	153		35	239	109
	COF-103	3530	4630	152/140[b]	4.4	35	298	110,111
Mg_2(DHTP)	Mg-MOF-74	1332		149	18.5	35	289	36
	COF-1	1230		148	6.2	35	298	110
$Cu_3(H_2O)_3$(BTEI)	PCN-61	3000	4600	145		35	298	47
$Co_2(BDC)_2$(DABCO)		1600	2300	140		35	289	26
$Zn_2(BDC)_2$(DABCO)		1450		137	26	35	289	112
	COF-102	3620	4650	127/140[b]	3.9	35	298	110,111
$Zn_4O(DBDC)_3$	IRMOF-3	2446	3062	120		36	289	7
$Cr_3OF(BTC)_2$	MIL-100	1900	2700	119		35	289	48
PAF	PPN-4	6461	10 063	117		35	295	45
$Zn_4O(BTB)_3$	MOF-177	4750	5640	116	4.4	35	298	31
Al(OH)(NDC)	DUT-4	1308	1996	114		35	303	113
Cr_3OF(BDC)	MIL-101	4230	5900	110		35	289	48
$Cu_3(H_2O)_3$(NTEI)		4000	4600	110	14.5	35	298	47
	COF-6	1050		110/150[b]	7.0	35	298	110
$Zn_4O(BDC)_3$	MOF-5 (IRMOF-1)	2296	3840	109	12.2	36	289	24
Zn_9O_3(2,7-NDC)$_6$		901	1281	107		50	289	114
Al(OH)(BPDC)	DUT-5	1613	2335	105		35	303	113
$Cu_3(H_2O)_3$(PTEI)	PCN-68	5109	6033	99		35	298	47
$Zn_4O(NDC)_3$	IRMOF-8	4182		90	9.2	35	298	6
	COF-8	1350	1400	94/125[b]	6.3	35	298	110,111
Zn_4O(BBC)	MOF-200	4530	10 400	84		80	298	110,114 115
Co_2(4,4′-BPY)$_2(NO_3)_4$				83		30	298	19
Cu_2(PIA)$(NO_3)_4$				65		31	289	116
Cd_2(AZPY)$_3(NO_3)$		1500		60		36	289	30
	COF-10	1760	2080	58/125[b]	6.6	35	298	110,111
Activated carbon		1250–3000		200		35	298	18
Zeolites		260–590		87		35	298	12

[a] ADIP = 5,5′-(9,10-anthracenediyl)di-isophthalate; AZPY = 4,4′-azopyridine; BDC^- = 1,4-benzenedicarboxylate; $BPDC^-$ = 4,4′-biphenyldicarboxylate; bpy = bipyridine; H_3BTB^{2-} = 1,3,5-tris(4-carboxyphenyl)benzene); BTC = benzenetricarboxzylate; BTEI = 5,5′,5″-(benzene-1,3,5-triyltris(ethyne-2,1-diyl))triisophthalic acid; DABCO = 1,4-diazabicyclo[2.2.2]octane; DBDC = 1,2-dihydocyclobutabenzene-3,6-dicarboxylate; DHTP = 2,5-dihydroxyterephthalic acid; NDC = 2,6-naphthalenedicarboxylate; NTEI = 5,5′,5″-((nitrilotris(benzene-4,1-diyl))tris(ethyne-2,1-diyl)) triisophthalic acid; PIA = *N*-(pyridine-4-yl)isonicotinamide; PTEI = 5,5′-((5′-(4-((3,5-dicarboxyphenyl(ethynyl)phenyl)-[1,1′,3′,1″-terphenyl]4-4″-diyl)bis(ethyne-2,1-diyl))diisophthalic acid; PYZ = pyrazine; PZDC = pyrazine-2,3-dicarboxylate; SBTC = Trans-stilbene-3,3′,5,5′-tetracarboxylic acid; IRMOF = Isoreticular metal organic framework. [b] Simulated value.

contrast, replacement of these linkers with rigid organic linkers results in open structures with large pores and high rigidity. For example, MOF-5 (Zn_4O–BDC)[24] has Zn_4O^{6+} inorganic clusters joined to six rigid benzene-1,4-dicarboxylate (BDC) anion ligands in an octahedral array to form a robust porous cubic framework with a BET surface area of 2296 m^2 g^{-1} and a methane uptake of 109 v/v STP.[24] A framework is not restricted to one type of organic linker, two or more linkers can be used to build a framework structure.[25] Zn_2(1,4-BDC)$_2$dabco is an example of a mixed ligand system, where benzene-1,4-dicarboxylate (BDC) and 1,4-diazabicyclo[2.2.2]octane (dabco) are used to give a three-dimensional framework with high surface

View Article Online

Published on 09 July 2012. Downloaded by CSIRO Library Services on 23/11/2015 04:48:30.

area and relatively small pores (BET surface area of 1450 $m^2 g^{-1}$ and uptake of 137 v/v STP).[26]

In identifying the promising topology candidates for methane storage, it is the surface area, optimal pore volume, and pore size which are the most important attributes to be considered for achieving maximum methane uptake. Snurr and co-workers demonstrated a computational approach to generate all conceivable MOFs from a chemical library of 102 building blocks (based on known MOFs) to give over 137 953 hypothetical MOFs with simulated methane uptake at 35 bar and 298 K.[27] From all the possible topologies, the best hypothetical MOFs were those with pore sizes of 4 to 8 Å, where the pore size is big enough for one or two methane molecules.[27]

One must also consider the experimental conditions, or application environment, of the MOF during use as a gas storage material. MOFs with smaller pores show a higher uptake of gas at lower pressures and possess strong methane interactions (higher heat of adsorption), whilst MOFs with larger pores are better suited to high pressure gas uptake experiments, where there is a gradual filling of the pores to give a higher overall capacity with overall weaker methane interactions. Independent of low (1–40 bar) or high (40 to 200 bar) pressure conditions, effective gas storage occurs in smaller pore sizes and pore volumes, where stronger methane interactions occur. This interplay between pore size, pore volume and heat of adsorption is illustrated by Thornton *et al.*, who simulated magnesium decorated fullerene molecules in known MOFs.[28] Thornton *et al.* showed that impregnation of MOF pores with magnesium-decorated fullerenes can be used as a method to position exposed metal sites with high heats of gas adsorption within large surface area MOF materials. Although part of the methane-accessible MOF porosity is occupied by the fullerenes, methane capacity can be increased. This increase in capacity is related to the tunability of pore sizes *via* linker length in conjunction with an increase in adsorption enthalpy.

2.2 Ligand design

The design of the ligand can play an important role for methane storage. The most commonly reported ligand groups used to construct MOFs are carboxylic acids and heterocyclic compounds containing nitrogen donor atoms.[29] Fig. 2 provides a short list of commonly used ligands, some of which are commercially available.

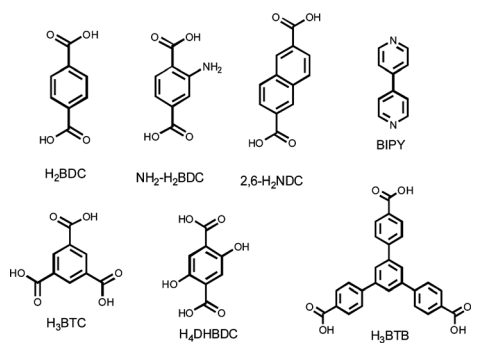

Fig. 2 Various carboxylic acid linkers used for MOF synthesis and a common nitrogen linker group 2,2′-bipyridine BIPY.

Introducing functional group(s) may increase the heat and strength of adsorption of the substrate; however, these functional groups may deleteriously alter the pore size and volume. A current strategy to avoid this is to enhance the ligand linker length, but not long enough to promote interpenetration.

The popular and commercially available Cu-BTC (also known as HKUST-1) MOF is constructed with the small 1,3,5-benzenetriscarboxylate ligand, with a BET surface area of 1502 $m^2 g^{-1}$ and a methane uptake of 160 v/v STP at 290 K and 35 bar.[30] MOF-177 is comprised of the extended phenyl ring link giving BTB (4,4′,4″-benzene-1,3,5-triyl-tribenzoate), which has a large BET surface area of 4750 $m^2 g^{-1}$ and a methane uptake of 116 v/v STP at 290 K and 35 bar.[31] These two examples illustrate the importance of pore volume to gas adsorption. A MOF which achieves reasonably high surface area without sacrificing pore volume is PCN-14, with a BET surface area of 1753 $m^2 g^{-1}$ and a methane uptake of 230 v/v STP at 290 K and 35 bar.[14] The anthracene based ligand provides the additional surface area for methane interactions without jeopardising pore size or volume.

Another area to consider with the ligand design is the hydrophobic properties available to enhance methane uptake. Due to the hydrophobic nature of methane, the incorporation of hydrophobic groups serves to increase methane interactions with the framework. The incorporation of hydrophobic groups, such as methyl and aromatic groups has been shown to increase methane uptake and additionally to improve MOF moisture stability.[32]

In summary, there are several strategies for designing ligands to produce MOFs optimised for methane storage, and it is clear that high surface area should not be the sole emphasis if the aim is to increase methane uptake, but instead pore volume and size must also be considered.

2.3 Open metal sites

Another strategy for enhancing methane uptake is to improve the methane binding energy (enthalpy of adsorption) in the MOF. This may be achieved by introducing coordinatively unsaturated "open" metal sites or by doping of the framework with metal centres.[6,33] Such methods have been shown to increase the enthalpy of adsorption of methane, as the metal sites are strongly cationic and can interact favourably with the adsorbate CH_4 molecule through Coulomb interactions.[34,35]

Several MOF compounds with open metal sites have been reported to exhibit exceptional methane uptake at room temperature and 35 bar. Some recent examples include M_2(dhtp)[36] (M = open metal, dhtp = 2,5-dihydroxyterephthalate; also known as MOF-74), Cu_3(bhb) (bhb = 3,3′,3″,5,5′,5″-benzene-1,3,5-triyl-hexabenzoate; also known as UTSA-20),[35] PCN-14,[14] Cu_2(sbtc) (sbtc – *trans*-stilbene-3,3′,5,5′-tetracarboxylate; also known as PCN-11)[34] and HKUST,[30] with the open metal site example compounds having methane uptakes of 150–190, 195, 230, 170, 160 v/v STP respectively at 298 K and 35 bar. Structurally all five examples contain the same dinuclear $M_2(CO_2)_4$ "paddlewheel" cluster topology, but differ in organic linkers and as a consequence give different pore sizes and volumes. The diversity allows for an evaluation of the roles that pore topology and linkers have on the effectiveness of an open metal site.

Zhou and co-authors[34] have determined the major methane adsorption sites in HKUST-1, PCN-11 and PCN-14 using

 This journal is © The Royal Society of Chemistry 2012

View Article Online

Published on 09 July 2012. Downloaded by CSIRO Library Services on 23/11/2015 04:48:30.

simulations and neutron powder diffraction experiments. They found that open metal sites bind to one methane molecule each through Coulomb interactions. They also discovered that it is the pore size of the pockets and cages which influence metal node – methane molecule interactions, through van der Waals interactions. The study concluded that open metal sites and methane-accessible small cages/pockets are favourable structural features and dominate the methane uptake.

It is observed from published work that the elongation of organic linkers with additional aromatic rings, such as in PCN-11, provides higher surface areas but offers little improvement to methane uptake. Nevertheless, these additional aromatic rings when positioned correctly can lead to the formation of small cages or areas of significant potential overlap for van der Waals interactions, as seen in PCN-14.

The doping of MOFs with alkali or transition metals is fast becoming an area of interest for hydrogen storage,[6,37] but there are limited examples of this strategy having been extended to methane storage.[6,38,39] The common alkali dopant is the lithium cation, as it is light in weight and has a strong binding energy for methane.[39,40] Simulation studies by Cao[39] have shown that lithium cations enhance methane uptake in covalent organic frameworks (discussed below) by improving the binding strength of methane to the substrate (London dispersions) and by inducing dipole interactions. The overall concept behind the doping strategy is to produce a MOF with moderate porosity in which the pore sizes are efficiently utilised through strong interactions between the gas molecule and the metal centre and doping is utilised to maximise the density of open metal sites.

2.4 Covalent organic frameworks

Covalent Organic Frameworks (COFs) are a class of porous compounds completely comprised of covalent bonds made entirely from light elements (H, B, C, N and O).[41–44] These organic polymers offer superior stability by replacing chemically susceptible coordination bonds with robust covalent bonds.[45] Like MOFs, COFs can exist as 2D and 3D networks. These materials have some distinct advantages over MOFs for applications in gas storage. One advantage is that COFs are light materials with very low density.[43] Another advantage is that they can be prepared from inexpensive and nontoxic building SBUs. A third advantage is that they possess high gravimetric surface areas.

One class of COFs is Porous Aromatic Framework (PAF) materials (also known as Porous Polymer Networks (PPNs)), in which a 3D network comprised mostly of carbon and hydrogen atoms give a diamond like structure (Fig. 3).[46] The linkers can be elongated with the introduction of additional aromatic rings but also can be shortened so they consist only of one aromatic ring per linker length (PAF-1). PAF-1 being the smallest structure of the family has a Langmuir surface area of 7100 $m^2 g^{-1}$, with the silicone derivative (PPN-4)[45] having a Langmuir surface area of 10 060 $m^2 g^{-1}$ which exceeds any MOF surface area, including PCN-68 and MIL-101 with respective Langmuir surface areas of 6030 $m^2 g^{-1}$ and 5900 $m^2 g^{-1}$.[46–48]

COFs and PAFs are attractive and versatile candidates for methane storage. Their low density, high surface area, pore sizes, tuneable frameworks, and accommodation of metal doping

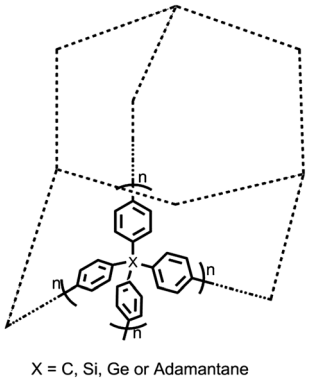

Fig. 3 Schematic diagram of porous aromatic framework, where X can be carbon, silicon, germanium or the group adamantane.

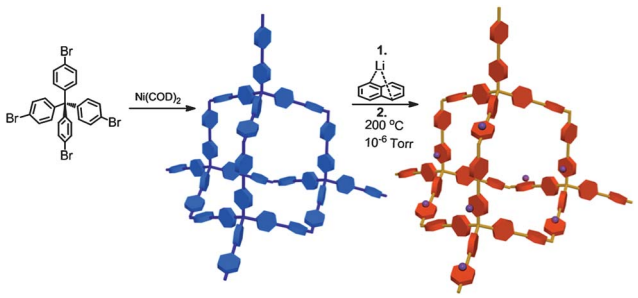

Fig. 4 Lithiation of PAF-1 leads to drastic increases in methane storage capacity.[38]

strategies make these materials prime candidates for consideration when designing a porous material suitable for methane storage. Konstas *et al.* recently reported a synthetic route for the lithiation of PAF-1 (Fig. 4) that results in a reduced and consequently activated PAF surface that increased the low pressure methane storage capacity of native PAF-1 by 71%.[38] Pore size distribution measurement and modelling results indicate a smaller pore size due to the incorporation of lithium ions in the framework, with pore size shrinking from 14 Å in PAF-1 to 11 Å in PAF-1 lithiated with 5 w/w Li. The combination of optimised porosity and enhanced adsorption enthalpies is shown to improve methane storage capacity.

3. Methane storage in adsorbent loaded tanks

The dominant technology for fuelling natural gas powered vehicles currently relies on storing the gas in a cylinder at pressures up to 300 bar.[20] Close to a million of these high pressure cylinders are used in passenger vehicles worldwide, but a few factors limit consumer acceptance of these systems. These technical difficulties are briefly outlined in the following paragraphs.[10,49,50]

The most even spread of stress and, therefore, the strongest and lightest tank results from using a cylindrical or spherical design. Unfortunately round tanks do not pack neatly into the space available in modern cars.[18]

Another technical disincentive to the use of CNG systems is cost. Firstly the purchase, installation and certification of the gas booster pumps required to fill low pressure reticulated gas into

View Article Online

Published on 09 July 2012. Downloaded by CSIRO Library Services on 23/11/2015 04:48:30.

high pressure CNG fuel tanks is expensive.[51] Secondly, the seamless steel or composite tanks required to safely contain gas under high pressure are more expensive than low pressure tanks such as those used to store LPG.

Adsorbed Natural Gas (ANG) fuel systems offer solutions to these two problems by either reducing the footprint for high-pressure systems or allowing sufficient range to be derived from low pressure systems. Most of the research work into ANG tanks focuses on activated carbon. Studies of MOF loaded adsorbent tanks for hydrocarbon fuel gasses remain scarce.[52] Despite concerted efforts in the 1980s by the Michigan Consolidated Gas Company,[53–55] commercial ANG systems have found limited markets to date.

Low pressure ANG systems may use simpler, cheaper tanks and equipment or even compact conformable tanks which are not available for CNG systems.[18] Several companies already produce multicellular tanks that combine the lower working pressures of ANG systems with the improved strength of smaller vessels. One such system is described by Mota.[49] U.S. DOE targets define the required storage performance of adsorbent systems at fill pressures of 35 bar.[8] Aside from reduced filling pump costs and more compact tanks, such pressures are similar to the maximum operating pressures found within automotive fluid systems and in LPG fuel tanks. This similarity may ease consumer concerns. For these reasons ANG system development is focused on low pressure applications rather than the potential for development of high-pressure/high-capacity tanks.

ANG systems may require adsorbents with characteristics tailored to their target storage pressure range. An excess of pores smaller than 7 Å may lead to a large proportion of the adsorbed gas unable to be desorbed ("cushion gas").[56] Despite inherently low dead volumes,[57] as mentioned previously the low packing density of MOFs may greatly reduce their volumetric storage capacity.[52,58] Therefore, the packing density (bulk density) of the adsorbent, needs to be optimised before a material can be considered for use as an adsorbent. Properties such as crystallographic density may give a misleading prediction of a material's usefulness as an adsorbent.[50,59–61]

Natural gas is supplied to the consumer as a complex mixture containing less than 93% methane and as little as 85% of methane and ethane combined.[62,63] Water, heavier hydrocarbons and other material such as sulphur containing odorants may damage the adsorbent bed. For this reason a small guard bed of adsorbent is placed at the adsorbent tank's inlet. Impurities that are trapped during filling may be swept back out during discharge, especially if the guard bed is heated, thus minimising or eliminating the need for replacement of the guard bed.[53] Carbon-based adsorbents operating without a guard bed suffer significant performance losses after 100 fill/fuel cycles, losing half of their efficiency after 700 cycles (approximately 250 000 km).[64]

3.1 Tank filling and discharge

Filling performance targets for ANG fuel tanks aim to obtain an 80% refill in 5 minutes and to sustain cycling losses at or below 5% per 100 cycles.[18] A challenge to be overcome is the need to distribute heat to/from the centre of large cylindrical adsorption vessels.[53–55,65–67] Heating during filling results in lower filling capacity while cooling during emptying leads to lower discharge rates.[68] Solutions include slow filling of the tank overnight, accepting reduced storage during 'emergency' fast fills, or using a circulating gas filling system with an integral chiller.[69]

Adding a gas distribution tube to the centre of the tank changes the way that gas flows and allows better heat distribution during discharge.[70] Electrical heating may be used to aid the delivery fuel gas from ANG tanks[53–55] and studies have shown that the use of internal heated water jackets may also be useful for this.[66] Studies of tank cooling during gas discharge from ANG tanks usually focus on the reduced storage efficiency of the tank as it cools.[68,70] As an example, flow rates of up to 15 L min^{-1}, corresponding to fuel use by a sub-compact car at cruising speed, have been used to test the effects of cooling during the discharge cycle of carbon filled ANG tanks.[70] Instantaneous fuel consumption by a large, high performance automobile under full throttle acceleration may be an order of magnitude greater than this. How ANG tanks will perform under such 'high demand' conditions is not clear. While much work has been done on ANG tanks using activated carbon adsorbents, the situation for MOFs is much less clear and will likely vary with the heat transmitting properties of the MOFs themselves.

3.2 Volumetric and gravimetric measurement of adsorption

The most common means of assessing the ability of a material to store a gas under pressure may be broadly classed as either volumetric or gravimetric adsorption measurements (Fig. 5).[71–74] New IUPAC guidelines for the reporting of gas/solid physisorption are being prepared.

Volumetry typically describes measurements of pressure variation with reference to a fixed, accurately known volume. The analysis measures the change in pressure within a sealed system containing the adsorbate and adsorbent in order to determine the amount of gas taken from the gas phase by the adsorbent.[74] Such measurements are better described as manometric to avoid confusion with true volumetric measurements. Gravimetry directly measures the mass of gas taken up by the adsorbent. When combined with the high precision and accuracy delivered by microbalances, this allows gravimetric measurement of adsorption/desorption processes to be performed with up to two orders of magnitude greater precision than with volumetric systems.

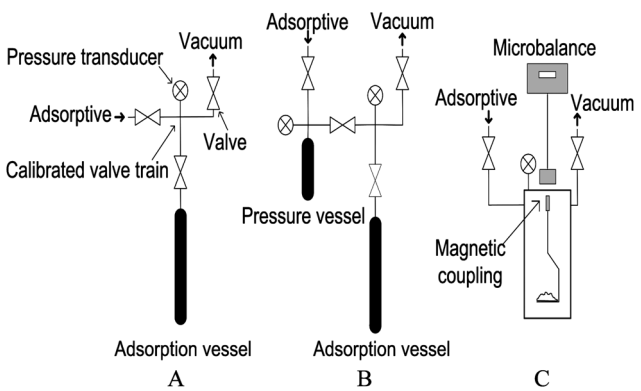

Fig. 5 (A) Simple volumetric apparatus, the valve train itself serves as the reference volume. (B) Volumetric apparatus with separate pressure vessel to act as a reference volume. (C) Gravimetric instrument.

 This journal is © The Royal Society of Chemistry 2012

View Article Online

Published on 09 July 2012. Downloaded by CSIRO Library Services on 23/11/2015 04:48:30.

The development of both techniques has been driven by fundamental research into adsorption phenomena and research into surface area analysis. While volumetry is historically the more common analysis, gravimetry has gained increasing acceptance with improvements in and reduced costs of weighing technology.[71–77]

For either method to be performed with sufficient accuracy various sources of experimental error must be minimised.[78] For both kinds of measurement sample outgassing is a source of error which will be discussed separately below. Precise temperature control is also essential,[79] generally the variation in temperature of the adsorption train, including any pressure reservoirs should be kept within ± 0.1–0.5 K.[74,76,79]

In volumetric measurements the main sources of error are: the measurement of the instrument's internal volume, pressure measurement, thermostasis or the measurement of temperature differentials across the instrument, leakage at high pressure and the measurement of the sample mass and dead volume. Errors in sample mass, in the determination of the instrument's internal volume, and in pressure measurements produce the most serious distortion of volumetric/manometric measurements.[77,78] Volumetric techniques typically use over/under pressures to drive equilibria and so may achieve equilibrium faster than gravimetric measurements.[76] Systems that take an impractically long time to come to equilibrium may use a fixed "technical equilibrium" time, based on a minimal amount of residual adsorption per unit time.[76,77] For gravimetric systems the main source of error is the measurement of the instrument's internal volume, which is subject to the same measurement errors that affect volumetric systems.[76,78] A significant advantage of gravimetric instruments is that they allow the sample to be weighed during the out gassing process. This feature allows errors in the sample mass to be minimised. Gravimetric measurements require a buoyancy correction to be applied which is the equivalent of the dead-volume correction required in volumetric measurements. A key disadvantage in using gravimetric systems to measure the performance of adsorbent materials is that the temperature of the adsorbent cannot be directly measured. This means that the measurement of adsorption/desorption behaviour on larger volumes of adsorbents, (where heating effects are likely to be more significant), or at high or low temperatures[74] are difficult to achieve on a gravimetric apparatus. For either technique it has been suggested that, using conventional equipment, sample sizes should be restricted to having surface areas in the range of 20–50 m^2 (*i.e.* ~50 mg for a 500 m^2 g^{-1} sample) to avoid problems with heat transfer.[72]

Scale-up testing of any new high performance material will generally require the use of specialised volumetric test equipment, while accurate screening and characterisation of candidate materials will be best performed using gravimetric techniques.[59,60]

4. Assessment of methane storage performance

4.1 Enthalpy of adsorption

The performance of any adsorptive process is directly determined by the quality of the adsorbent. It is generally accepted that an adsorbent with a sufficiently high specific volume/surface area and adsorption affinity is necessary for optimised adsorption capacity.[9,80] However, a higher than optimal adsorption affinity will result in reduced gas delivery on board due to difficulty in desorbing the adsorbate species, and a lower than optimal adsorption affinity will result in weak binding between gas molecules and adsorbent and will lead to suboptimal adsorption capacity. Therefore, an analysis of the adsorption affinity or isosteric enthalpy of adsorption is necessary to assess the adsorbent's performance for on board storage.

4.1.1 Low surface coverage of adsorbate: Henry law equation. At low coverage, adsorption of gases can be treated as a monolayer and therefore, the Langmuir isotherm may be used,

$$\frac{q}{q_s} = \frac{bp}{1+bp} \quad (1)$$

where, q_s is the saturated limit adsorbed, b is the constant in Langmuir equation and p is the pressure.

At zero coverage, the adsorption isotherm reduces to Henry's law

$$\lim_{p\to 0}\left(\frac{q}{p}\right) = bq_s = k \quad (2)$$

where, k is the Henry's law constant and should vary with temperature in accordance with the van't Hoff equation:

$$k = k_0 \exp\left(\frac{-\Delta H}{RT}\right) \quad (3)$$

where k_0 is the pre-exponential parameter of the van't Hoff equation, ΔH is the enthalpy of adsorption, R is the universal gas constant and T is temperature.

However, it is worth mentioning that constants derived by matching the experimental data to these models may lack physical significance when the data are extended over the entire pressure range because the prerequisites for these models may not be valid across such a broad range of pressures.[81] Also, due to this limitation, the values of q_s obtained are generally lower than the true saturation coverage.[82] However, it is also worth bearing in mind that, for a light gas such as methane that is weakly interacting with the adsorbent, the Langmuir model provides sufficient accuracy over a wide range of pressures.[9] Virial fitting methods have also been employed as another means for determining zero-coverage enthalpies, an approach where the isotherms recorded at differing temperatures are fit simultaneously by a floating number of virial coefficients, allowing greater accuracy in the extrapolation back to zero-coverage values.[83]

4.1.2 High surface coverage of adsorbate: Clausius–Clapeyron equation. As we mentioned above, the Henry law equation shows the theoretical limits at pressures approaching zero or a low gas adsorbate coverage where adsorbate and adsorbent interaction dominates. In reality, the enthalpy of adsorption is not only due to interaction between a gas molecule and an adsorbent surface atom but also cooperative interactions between gas molecules adsorbed on the adsorbent surface.[84] Therefore, the differential enthalpy of adsorption will vary with coverage or amount of gas adsorbed, especially when the adsorbent surface is heterogeneous.

View Article Online

Published on 09 July 2012. Downloaded by CSIRO Library Services on 23/11/2015 04:48:30.

There are different ways to calculate this average heat of adsorption.[9,81,85–89] The simplest and most widely applied estimation of this average heat of adsorption is calculated by the Clausius–Clapeyron equation,[9,90,91] where fitting a polynomial curve to recorded data to derive a given pressure for a specific gas uptake at closely related temperatures allows the slope of a plot of ln P *vs.* $1/T$ to give the enthalpy of adsorption as a function of coverage.

4.2 Characterisation of kinetic fundamentals

For the application of methane storage materials, the time to fill and empty the adsorbent is crucial. For example, in the automotive industry, filling time is regarded as a barrier to the take up of alternative fuels, and the desorption rate must be sufficient to meet the fuel consumption demands of the vehicle. Therefore the characterisation of the adsorption kinetics within candidate materials should be of great importance, but is rarely reported. Fundamentally, studying molecular diffusion in nanoporous materials provides unique insights into the host–guest interaction and the interrelation between pore structure and propagation rates. On the other hand, the rate of molecular propagation is one of the decisive quantities affecting the effectiveness of technical processes on application of the nanoporous materials.[92] It becomes especially important when the system is in a non-equilibrium state, which is typical of most of the industrially used adsorption processes today. Therefore, molecular diffusion measurements both at microscopic and macroscopic scales, is of essential significance. There are different methods available to measure the diffusion coefficients, for example, pulsed field gradient nuclear magnetic resonance (PFG NMR),[93–95] quasi-elastic neutron scattering (QENS),[96–98] volumetric,[99,100] gravimetric[97] and chromatographic methods[101] for either non-equilibrium and equilibrium conditions. QENS is able to trace molecular displacements below a few nanometers and can give the elementary process of diffusion at submicroscopic scale under equilibrium conditions, whereas PFG NMR, with a useful working range typically between 100 nm and 100 μm, is able to observe both intracrystalline and long-range diffusion.[92] Volumetric, gravimetric and chromatographic techniques are usually carried out under non-equilibrium conditions where a finite concentration gradient exists.

However, for the experimentalist, collection of kinetic data in conjunction with adsorption measurements is the most convenient method. It is possible to utilise transducers fitted for the purpose of determining adsorption equilibrium to reveal the rate of adsorption as equilibrium is reached, and from this, kinetic parameters can be elucidated. In fact, this approach has been employed as a standard in gas separation membrane research, where diffusion parameters have long been determined through adsorption experiments.[102–104]

5. Applications and outlook

The use of MOFs in natural gas-based applications is in the early stages, and to date has largely been limited to adsorptive storage for vehicular applications. There is a great potential to expand these early promising outcomes much further, given the numerous uses of natural gas where an adsorbent may provide an advantage. For example, MOF adsorbents could be used in concert with any existing LNG system to minimise boil-off losses, or to capture and store methane emitted from biological processes such as fermentation. MOFs are already finding application for selective gas adsorption, which has particular relevance for natural gas processing, where high levels of carbon dioxide or nitrogen may often be found in native reserves.

However, there exist many research challenges that must be addressed as part of the broader development of these materials for applications. Large scale synthetic routes that deliver high purity products at low costs are paramount. Whilst there are reports of some MOFs being able to be prepared at the scale of hundreds of kilograms (see Introduction), many MOFs do not scale well under the present synthetic pathways, with their purity decreasing at larger reaction sizes. Novel routes that may involve microwaves, electroplating or nucleating are needed to aid large scale usage. Stability to the often harsh target environmental conditions should be a key aspect in future developments, and considered at all points in the developments cycle. There remains some distance before MOFs are cost competitive, although on a cost-per-unit performance measure the outlook is more promising. Low cost starting materials and low energy reaction pathways will also ease inherent costs, with other costs lessening during progress along the supply chain. Another key challenge is to develop approaches for the handling of MOFs within target applications. Many MOFs will need to be periodically regenerated, or may have a defined natural lifetime for usage and the various routes for achieving this with a low impact should be a key area of consideration for researchers.

In summary, MOFs have remarkable potential for the high density storage of natural gas. Their ultrahigh porosity and tuneable surface chemistry renders them as smart materials in this field, able to be tailored to the specific demands of a storage application, with the associated target temperatures, pressures, and kinetics. They presently hold the highest storage capacities for any material, making their further development for applications a fruitful area of research with a large potential commercial benefit.

Notes and references

1 J. Pucker, R. Zwart and G. Jungmeier, *Biomass Bioenergy*, 2012, **38**, 95–101.
2 Adapted from: http://www.iea.org/stats/index.asp.
3 M. Diesendorf, D. Lamb, J. Matthews and G. Pearman, in *A roadmap to alternative fuels in Australia: Ending our dependence on oil*, Jamison Group, NRMA Motoring and Services, Sydney, 2008.
4 M. Diesendorf, D. Lamb, J. Matthews, N. Burke and G. Pearman, in *Fuelling future passenger vehicle use in Australia*, Jamison Group, NRMA Motoring and Services, Sydney, 2010, p. 130.
5 J. J. Wozniak, J. A. Ecker and R. J. Hildebrand, *Johns Hopkins APL Tech. Dig.*, 1995, **16**, 95–100.
6 R. B. Getman, Y.-S. Bae, C. E. Wilmer and R. Q. Snurr, *Chem. Rev.*, 2012, **112**, 703–723.
7 M. Eddaoudi, J. Kim, N. Rosi, D. Vodak, J. Wachter, M. O'Keeffe and O. M. Yaghi, *Science*, 2002, **295**, 469–472.
8 T. Burchell and M. Rodgers, *SAE Tech. Pap. Ser.*, 2000, 2201–2205.
9 S. K. Bhatia and A. L. Myers, *Langmuir*, 2006, **22**, 1688–1700.
10 D. Lozano-Castello, J. Alcaniz-Monge, M. A. de la Casa-Lillo, D. Cazorla-Amoros and A. Linares-Solano, *Fuel*, 2002, **81**, 1777–1803.
11 A. Celzard and V. Fierro, *Energy Fuels*, 2005, **19**, 573–583.
12 V. C. Menon and S. Komarneni, *J. Porous Mater.*, 1998, **5**, 43–58.

 This journal is © The Royal Society of Chemistry 2012

View Article Online

Published on 09 July 2012. Downloaded by CSIRO Library Services on 23/11/2015 04:48:30.

13 X.-S. Wang, S. Ma, K. Rauch, J. M. Simmons, D. Yuan, X. Wang, T. Yildirim, W. C. Cole, J. J. Lapez, A. de Meijere and H.-C. Zhou, *Chem. Mater.*, 2008, **20**, 3145–3152.
14 S. Q. Ma, D. F. Sun, J. M. Simmons, C. D. Collier, D. Q. Yuan and H. C. Zhou, *J. Am. Chem. Soc.*, 2008, **130**, 1012–1016.
15 P. Falcaro, A. J. Hill, K. M. Nairn, J. Jasieniak, J. I. Mardel, T. J. Bastow, S. C. Mayo, M. Gimona, D. Gomez, H. J. Whitfield, R. Ricca, A. Patelli, B. Marmiroli, H. Amenitsch, T. Colson, L. Villanova and D. Buso, *Nat. Commun.*, 2011, **2**, 237.
16 N. L. Campbell, R. Clowes, L. K. Ritchie and A. I. Cooper, *Chem. Mater.*, 2009, **21**, 204–206.
17 Q. Min Wang, D. Shen, M. Bulow, M. Ling Lau, S. Deng, F. R. Fitch, N. O. Lemcoff and J. Semanscin, *Microporous Mesoporous Mater.*, 2002, **55**, 217–230.
18 J. Wegrzyn and M. Gurevich, *Appl. Energy*, 1996, **55**, 71–83.
19 M. Kondo, T. Yoshitomi, H. Matsuzaka, S. Kitagawa and K. Seki, *Angew. Chem., Int. Ed. Engl.*, 1997, **36**, 1725–1727.
20 W. Zhou, *Chem. Rec.*, 2010, **10**, 200–204 and references within.
21 M. Eddaoudi, D. B. Moler, H. Li, B. Chen, T. M. Reineke, M. O'Keeffe and O. M. Yaghi, *Acc. Chem. Res.*, 2001, **34**, 319–330.
22 D. Zhao, D. J. Timmons, D. Yuan and H.-C. Zhou, *Acc. Chem. Res.*, 2011, **44**, 123–133.
23 O. M. Yaghi, M. O'Keeffe, N. W. Ockwig, H. K. Chae, M. Eddaoudi and J. Kim, *Nature*, 2003, **423**, 705–714.
24 H. Li, M. Eddaoudi, M. O'Keeffe and O. M. Yaghi, *Nature*, 1999, **402**, 276–279.
25 C. Janiak and J. K. Vieth, *New J. Chem.*, 2010, **34**, 2366–2388.
26 D. N. Dybtsev, H. Chun and K. Kim, *Angew. Chem., Int. Ed.*, 2004, **43**, 5033–5036.
27 C. E. Wilmer, M. Leaf, C. Y. Lee, O. K. Farha, B. G. Hauser, J. T. Hupp and R. Q. Snurr, *Nat. Chem.*, 2012, **4**, 83–89.
28 A. W. Thornton, K. M. Nairn, J. M. Hill, A. J. Hill and M. R. Hill, *J. Am. Chem. Soc.*, 2009, **131**, 10662–10669.
29 F. A. Almeida Paz, J. Klinowski, S. M. F. Vilela, J. P. C. Tomé, J. A. S. Cavaleiro and J. Rocha, *Chem. Soc. Rev.*, 2012, **41**, 1088–1110.
30 S. Ma and H.-C. Zhou, *Chem. Commun.*, 2010, **46**, 44–53.
31 H. K. Chae, D. Y. Siberio-Perez, J. Kim, Y. Go, M. Eddaoudi, A. J. Matzger, M. O'Keeffe and O. M. Yaghi, *Nature*, 2004, **427**, 523–527.
32 D. Ma, Y. Li and Z. Li, *Chem. Commun.*, 2011, **47**, 7377–7379.
33 X. Lin, I. Telepeni, A. J. Blake, A. Dailly, C. M. Brown, J. M. Simmons, M. Zoppi, G. S. Walker, K. M. Thomas, T. J. Mays, P. Hubberstey, N. R. Champness and M. Schröder, *J. Am. Chem. Soc.*, 2009, **131**, 2159–2171.
34 H. Wu, J. M. Simmons, Y. Liu, C. M. Brown, X.-S. Wang, S. Ma, V. K. Peterson, P. D. Southon, C. J. Kepert, H.-C. Zhou, T. Yildirim and W. Zhou, *Chem.–Eur. J.*, 2010, **16**, 5205–5214.
35 Z. Guo, H. Wu, G. Srinivas, Y. Zhou, S. Xiang, Z. Chen, Y. Yang, W. Zhou, M. O'Keeffe and B. Chen, *Angew. Chem., Int. Ed.*, 2011, **50**, 3178–3181.
36 H. Wu, W. Zhou and T. Yildirim, *J. Am. Chem. Soc.*, 2009, **131**, 4995–5000.
37 S. S. Han and W. A. Goddard, *J. Am. Chem. Soc.*, 2007, **129**, 8422–8423.
38 K. Konstas, J. W. Taylor, A. W. Thornton, C. M. Doherty, W. X. Lim, T. J. Bastow, D. F. Kennedy, C. D. Wood, B. J. Cox, J. M. Hill, A. J. Hill and M. R. Hill, *Angew. Chem., Int. Ed.*, 2012, 6639–6642.
39 J. Lan, D. Cao and W. Wang, *Langmuir*, 2010, **26**, 220–226.
40 A. Mavrandonakis, E. Tylianakis, A. K. Stubos and G. E. Froudakis, *J. Phys. Chem. C*, 2008, **112**, 7290–7294.
41 H. M. El-Kaderi, J. R. Hunt, J. L. Mendoza-Cortes, A. P. Cote, R. E. Taylor, M. O'Keeffe and O. M. Yaghi, *Science*, 2007, **316**, 268–272.
42 A. I. Cooper, *Adv. Mater.*, 2009, **21**, 1291–1295.
43 A. P. Coté, A. I. Benin, N. W. Ockwig, M. O'Keeffe, A. J. Matzger and O. M. Yaghi, *Science*, 2005, **310**, 1166–1170.
44 S. Kitagawa, R. Kitaura and S.-i. Noro, *Angew. Chem., Int. Ed.*, 2004, **43**, 2334–2375.
45 D. Yuan, W. Lu, D. Zhao and H.-C. Zhou, *Adv. Mater.*, 2011, **23**, 3723–3725.
46 T. Ben, H. Ren, S. Ma, D. Cao, J. Lan, X. Jing, W. Wang, J. Xu, F. Deng, J. M. Simmons, S. Qiu and G. Zhu, *Angew. Chem., Int. Ed.*, 2009, **48**, 9457–9460.
47 D. Yuan, D. Zhao, D. Sun and H.-C. Zhou, *Angew. Chem., Int. Ed.*, 2010, **49**, 5357–5361.
48 G. Férey, C. Mellot-Draznieks, C. Serre, F. Millange, J. Dutour, S. Surblé and I. Margiolaki, *Science*, 2005, **309**, 2040–2042.
49 J. P. B. Mota, in *Recent Advances in Adsorption Processes for Environmental Protection and Security*, ed. J. P. Mota and S. Lyubchik, Springer, Dordrecht, 2008, pp. 177–192.
50 M. Tagliabue, C. Rizzo, R. Millini, P. D. C. Dietzel, R. Blom and S. Zanardi, *J. Porous Mater.*, 2011, **18**, 289–296.
51 P. C. Flynn, *Energy Policy*, 2002, **30**, 613–619.
52 U. Mueller, M. Schubert, F. Teich, H. Puetter, K. Schierle-Arndt and J. Pastre, *J. Mater. Chem.*, 2006, **16**, 626–636.
53 L. J. Engel and J. W. Turko, *Ger. Pat.*, 3515221 A1, 1985.
54 L. J. Engel and J. W. Turko, *Ger. Pat.*, 3515220 A1, 1985.
55 L. J. Engel and J. W. Turko, *US. Pat.*, 4522159 A, 1985.
56 J. Sun, T. D. Jarvi, L. F. Conopask, S. Satyapal, M. J. Rood and M. Rostam-Abadi, *Energy Fuels*, 2001, **15**, 1241–1246.
57 I. Senkovska and S. Kaskel, *Microporous Mesoporous Mater.*, 2008, **112**, 108–115.
58 L. J. Murray, M. Dinca and J. R. Long, *Chem. Soc. Rev.*, 2009, **38**, 1294–1314.
59 J. P. Marco-Lozar, J. Juan-Juan, F. Suarez-Garcia, D. Cazorla-Amoros and A. Linares-Solano, *Int. J. Hydrogen Energy*, 2012, **37**, 2370–2381.
60 A. Dailly and E. Poirier, *Energy Environ. Sci.*, 2011, **4**, 3527–3534.
61 Z. Jia, H. Li, Z. Yu, P. Wang and X. Fan, *Mater. Lett.*, 2011, **65**, 2445–2447.
62 N. G. Q. S. Committee AG-010, Standards Australia, 2011.
63 A. J. Kidnay and W. R. Parrish, *Fundamentals of Natural Gas Processing*, Taylor and Francis, Boca Raton, 2006.
64 O. Pupier, V. Goetz and R. Fiscal, *Chem. Eng. Process.*, 2005, **44**, 71–79.
65 K. R. Matranga, A. Stella, A. L. Myers and E. D. Glandt, *Sep. Sci. Technol.*, 1992, **27**, 1825–1836.
66 W. S. Loh, K. A. Rahman, A. Chakraborty, B. B. Saha, Y. S. Choo, B. C. Khoo and K. C. Ng, *J. Chem. Eng. Data*, 2010, **55**, 2840–2847.
67 S. C. Hirata, P. Couto, L. G. Lara and R. M. Cotta, *Int. J. Therm. Sci.*, 2009, **48**, 1176–1183.
68 S. Biloe, V. Goetz and S. Mauran, *AIChE J.*, 2001, **47**, 2819–2830.
69 J. P. B. Mota, A. E. Rodrigues, E. Saatdjian and D. Tondeur, *Carbon*, 1997, **35**, 1259–1270.
70 K. J. Chang and O. Talu, *Appl. Therm. Eng.*, 1996, **16**, 359–374.
71 J. U. Keller and R. Staudt, *Gas Adsorption Equilibria: Experimental Methods and Adsorptive Isotherms*, Springer, Boston, 2005.
72 F. Rouquerol, J. Rouquerol and K. Sing, *Adsorption by Powders and Porous Solids. Principles, Methodology and Applications*, Academic Press, London, 1999.
73 D. Young and A. Crowell, *Physical Adsorption of Gasses*, Butterworths, London, 1962.
74 K. S. W. Sing, D. H. Everett, R. A. W. Haul, L. Moscou, R. A. Pierotti, J. Rouquerol and T. Siemieniewska, *Pure Appl. Chem.*, 1985, **57**, 603–619.
75 J. U. Keller, H. Rave, M. Seelbach and R. Staudt, *Adsorpt. Sci. Technol.*, 2000, 329–335.
76 D. P. Broom, *Int. J. Hydrogen Energy*, 2007, **32**, 4871–4888.
77 J. U. Keller, E. Robens and C. D. von Hohenesche, *Characterization of Porous Solids VI*, 2002, vol. 144, pp. 387–394.
78 Y. Belmabkhout, M. Frere and G. De Weireld, *Meas. Sci. Technol.*, 2004, **15**, 848–858.
79 B. M. Krooss, F. van Bergen, Y. Gensterblum, N. Siemons, H. J. M. Pagnier and P. David, *Int. J. Coal Geol.*, 2002, **51**, 69–92.
80 L. Myers, *Chem. Eng.*, 1992, **47**, 1569–1579.
81 D. M. Ruthven, *Principles of Adsorption and Adsorption Processes*, John Wiley & Sons, 1984.
82 S. Pakseresht, M. Kazemeini and M. M. Akbarnejad, *Sep. Purif. Technol.*, 2002, **28**, 53–60.
83 L. Czepirsky and J. Jagiello, *Chem. Eng. Sci.*, 1989, **44**, 797.
84 C. Nguyen and D. D. Do, *J. Phys. Chem. B*, 1999, **103**, 6900–6908.
85 Z. J. Liu, D. D. Do and D. Nicholson, *J. Colloid Interface Sci.*, 2011, **361**, 278–287.
86 P. Kowalczyk, *Phys. Chem. Chem. Phys.*, 2012, **14**, 2784–2790.
87 D. D. Do, D. Nicholson and C. Y. Fan, *Langmuir*, 2011, **27**, 14290–14299.
88 R. Yang, *Adsorbents: Fundamentals and Applications*, John Wiley and Sons, 2003.

View Article Online

Published on 09 July 2012. Downloaded by CSIRO Library Services on 23/11/2015 04:48:30.

89 M. R. Bonilla, J. S. Bae, T. X. Nguyen and S. K. Bhatia, *J. Phys. Chem. C*, 2010, **114**, 16562–16575.
90 S. Himeno, T. Komatsu and S. Fujita, *J. Chem. Eng. Data*, 2005, **50**, 369–376.
91 G. Yushin, R. Dash, J. Jagiello, J. E. Fischer and Y. Gogotsi, *Adv. Funct. Mater.*, 2006, **16**, 2288–2293.
92 J. Karger, *Adsorpt. J. Int. Adsorpt. Soc.*, 2003, **9**, 29–35.
93 L. F. Gladden, *Chem. Eng. Sci.*, 1994, **49**, 3339–3408.
94 M. Krutyeva, S. Vasenkov, X. Yang, J. Caro and J. Kaerger, *Microporous Mesoporous Mater.*, 2007, **104**, 89–96.
95 U. Hong, J. Karger, B. Hunger, N. N. Feoktistova and S. P. Zhdanov, *J. Catal.*, 1992, **137**, 243–251.
96 H. Jobic, *J. Mol. Catal. A: Chem.*, 2000, **158**, 135–142.
97 J. Wloch, *Microporous Mesoporous Mater.*, 2003, **62**, 81–86.
98 Y. X. Yang, C. M. Brown, C. X. Zhao, A. L. Chaffee, N. Burke, D. Y. Zhao, P. A. Webley, J. Schalch, J. M. Simmons, Y. Liu, J. H. Her, C. E. Buckley and D. A. Sheppard, *Carbon*, 2011, **49**, 1305–1317.
99 R. S. Pillai, G. Sethia and R. V. Jasra, *Ind. Eng. Chem. Res.*, 2010, **49**, 5816–5825.
100 G. Sethia, R. S. Pillai, G. P. Dangi, R. S. Somani, H. C. Bajaj and R. V. Jasra, *Ind. Eng. Chem. Res.*, 2010, **49**, 2353–2362.
101 P. S. Barcia, J. A. C. Silva and A. E. Rodrigues, *Microporous Mesoporous Mater.*, 2005, **79**, 145–163.
102 S. Keskin and D. S. Sholl, *Langmuir*, 2009, **25**, 11786–11795.
103 S. E. Jee and D. S. Sholl, *J. Am. Chem. Soc.*, 2009, **131**, 7896–7904.
104 S. Keskin and D. S. Sholl, *J. Phys. Chem. C*, 2007, **111**, 14055–14059.
105 K. Seki and W. Mori, *Langmuir*, 2002, 1380–1385.
106 S. Bourrelly, P. L. Llewellyn, C. Serre, F. Millange, T. Loiseau and G. Férey, *J. Am. Chem. Soc.*, 2005, **127**, 13519–13521.
107 C. Tan, S. Yang, N. R. Champness, X. Lin, A. J. Blake, W. Lewis and M. Schröder, *Chem. Commun.*, 2011, **47**, 4487–4489.
108 S.-i. Noro, S. Kitagawa, M. Kondo and K. Seki, *Angew. Chem., Int. Ed.*, 2000, **39**, 2081–2084.
109 K. Seki and W. Mori, *J. Phys. Chem. B*, 2002, **106**, 1380–1385.
110 J. L. Mendoza-Cortes, T. A. Pascal and W. A. Goddard, *J. Phys. Chem. A*, 2011, **115**, 13852–13857.
111 H. Furukawa and O. M. Yaghi, *J. Am. Chem. Soc.*, 2009, **131**, 8875–8883.
112 H. Kim, D. G. Samsonenko, S. Das, G.-H. Kim, H.-S. Lee, D. N. Dybtsev, Ea. Berdonosova and K. Kim, *Chem.–Asian J.*, 2009, **4**, 886–891.
113 I. Senkovska, F. Hoffmann, M. Fröba, J. Getzschmann, W. Böhlmann and S. Kaskel, *Microporous Mesoporous Mater.*, 2009, **122**, 93–98.
114 M. Park, D. Moon, J. W. Yoon, J.-S. Chang and M. S. Lah, *Chem. Commun.*, 2009, 2026–2028.
115 H. Furukawa, N. Ko, Y. B. Go, N. Aratani, S. B. Choi, E. Choi, A. O. Yazaydin, R. Q. Snurr, M. O'Keeffe, J. Kim and O. M. Yaghi, *Science*, 2010, **329**, 424–428.
116 M. Kondo, T. Okubo, A. Asami, S.-i. Noro, T. Yoshitomi, S. Kitagawa, T. Ishii, H. Matsuzaka and K. Seki, *Angew. Chem., Int. Ed.*, 1999, **38**, 140–143.

 This journal is © The Royal Society of Chemistry 2012